Department of the Navy
Bureau of Ordnance
Contract NOrd-16200
Task 1

FORCES ON COMPOSITE BODIES IN FULL CAVITY FLOW

R. L. Waid

Hydrodynamics Laboratory
CALIFORNIA INSTITUTE OF TECHNOLOGY
Pasadena, California

Report No. E-73.8 September 1957

Department of the Navy
Bureau of Ordnance
Contract NOrd-16200
Task 1

FORCES ON COMPOSITE BODIES IN FULL CAVITY FLOW

R. L. Waid

Hydrodynamics Laboratory
California Institute of Technology
Pasadena, California

Report No. E-73.8

September 1957

ABSTRACT

Experimental force measurements on several truncated cone-cylinder bodies operating in full cavity flow are reported. Lift, drag and pitching moment coefficients and the center of pressure are presented as functions of angle of attack for cavitation numbers from 0.02 to 0.06. The lift and drag coefficients are compared with predicted results which are based on the summation of the forces on individual body components. Discrepancies between the experimental and the predicted results are discussed.

INTRODUCTION

The design of stable, high speed cavity running missiles requires an optimum combination of body components to provide the required stability with the minimum drag. To this end an extensive program has been conducted at the Hydrodynamics Laboratory[1]* to obtain basic information about the various aspects of composite missiles operating in full cavity flow. The forces and moments acting on cavity producing noses have been evaluated[2-5]. The shapes of the cavities produced by these noses have been determined[3,4,6]. The techniques of sustaining cavities by the use of air has been developed[7]. Flat surface planing forces have been obtained for cylindrical bodies[8], conical bodies[9], rings[10], and complex bodies with fins and shroud rings[11]. Forces on cylindrical bodies planing on curved surfaces have been studied at both low[12,13] and high[13] free stream cavitation numbers. Planing forces on a complex body with fins and shroud rings have also been obtained on a curved surface at low cavitation numbers[14]. Forces on a streamlined nose, finned afterbody configuration in full cavity flow have also been reported[15].

This report presents the results of a program to experimentally determine and to analytically predict the forces on a basic type of configuration in full cavity flow. The three models tested are of a family of truncated cone-cylinder bodies which have been tested elsewhere for water entry characteristics[16,17]. The cavity producing surface or nose of the model was the truncated face of the cone while the cylinder formed the model afterbody. The lift, drag and pitching moment on the composite model was obtained as a function of the pitch angle of the model for several cavitation numbers. The model pitch was varied from 0 to +15.5 degrees while the cavitation numbers ranged from 0.02 to 0.06. The test program was conducted in the Free Surface Water Tunnel at a free stream velocity of 26 fps, using air sustained cavities[7].

In addition to the full cavity tests two of the models were also planed upon the flat surface of the water to obtain a comparison between the cone-cylinder planing data and the cylinder planing data[13] which were used for

---

* Superscripts denote references in Bibliography.

predicting the composite force coefficients. The planing tests were conducted at 26 fps free stream velocity for an angle of attack range from 0 to +15.5 degrees.

The predicted lift and drag coefficients were obtained by combining nose force data[2] with cavity shape data[6] and adding the afterbody forces as corrected for lateral surface curvature[13]. The afterbody forces were computed for both an entirely cylindrical afterbody and for the cone-cylinder afterbody as evaluated by the above mentioned planing tests.

EXPERIMENTAL PROCEDURES

The truncated cone cylinder models are shown in Fig. 1, while the model dimensions in terms of the base diameter (1.500 inches) are presented in Fig. 2. The model designation is A-4-5, A-4-10, E-4-5. The first integer refers to the overall length-to-diameter ratio with A = 5.33 and E = 5.83. The second integer refers to the nose-to-base diameter ratio which was 0.37 for these tests and is designated by the numeral 4. The last integers refer to the half-angle of the conical portion of the body and are designated in degrees.

The models were installed on a new pitching strut and shield assembly which was attached to the existing three-component force balance, Fig. 3. The entire model, strut-shield, and balance combination, were mounted on the elevating mechanism of the Free Surface Water Tunnel. The pitching strut was designed so that the models could be remotely pitched while other test variables were unchanged.

The force balance zeros were obtained with the model and strut above the water surface. The nominal adjustment of the cavitation number was obtained by setting the model at various submergences below the water surface and by adjusting the air flow into the cavity. One submergence level and one air flow setting were maintained for each test run. Because of the variations in gas entrainment from the cavity due to the deformation of the cavity by the model, the actual cavity pressure was measured and found to vary considerably during a run. Consequently the final force data are presented

along with the computed cavitation numbers. The measured forces were forward and aft lift and drag. From these three forces the total lift force, drag force, pitching moment and center of pressure were obtained. In addition to these recorded data, concurrent reference photographs were taken of the model and the flow for each test condition.

Two models of the A-4-10 configuration with different support points, Fig. 2, were tested to investigate possible tare effects due to spray impingement on the short unshielded portion of the strut inside of the cavity. Large planing angles of the afterbody were known to produce spray inside the cavity and differences between the observed data would thus suggest the magnitude of the spray induced tare force.

The planing afterbody tests were performed with the models attached to the same strut assembly as used for the cavity flow tests. The models were preset to angles of attack and the model elevation varied so that the model planed on the free surface. The force and photographic data were similar to those for the cavity tests.

EXPERIMENTAL RESULTS

The recorded experimental data were reduced to the following dimensionless coefficients:

$$\text{Drag coefficient, } C_D = \frac{\text{DRAG}}{\rho/2\, V^2 A}$$

$$\text{Lift coefficient, } C_L = \frac{\text{LIFT}}{\rho/2\, V^2 A}$$

$$\text{Pitching moment coefficient, } C_M = \frac{\text{PITCHING MOMENT}}{\rho/2\, V^2 A\, d}$$

$$\text{Center of pressure ratio, } \frac{L_1}{d} = \frac{\text{PITCHING MOMENT}}{d(\text{Drag} \sin\alpha + \text{Lift} \cos\alpha)}$$

$$\text{Cavitation number, } \sigma = \frac{P_o - P_k}{\rho/2\, V^2} \times 144$$

The symbols are defined in Table I and the sign conventions indicated in Fig. 4.

The force and moment coefficients together with the cavitation numbers for full cavity flow about model A-4-5 are presented in Figs. 5 and 6 as a function of pitch angle. Figures 7 and 8 present the data for the E-4-5 configuration, while Figs. 9 and 10 present the A-4-10 results. The data points obtained at a submergence of 0.25 feet are shown in these figures to illustrate the close spacing of the data points and the consistency of the measured data. The points were omitted from the other curves for simplicity. Normally an increase in submergence caused the nominal cavitation number to increase. However, it is noted in Fig. 5 that the submergence of 0.55 ft. for the A-4-5 model was run at a lower cavitation number than the 0.45 submergence. This was due to the increase in air flow required to maintain a suitable cavity at the greater depth.

The force and moment data seem to have a very systematic behavior. At small angles of attack the forces are only those acting on the nose of the model since the body was completely enclosed in the nose cavity as shown in Fig. 11. This figure shows a series of flow photographs for the A-4-5 model at 0.25 submergence. As the afterbody breaks through the cavity wall, the forces and moments increase rapidly, the center of pressure moves forward and the cavitation number starts to increase slightly. As the pitch angle increases further the forces and moments fluctuate several times and then tend to settle. The center of pressure became fairly constant at the higher angles while the cavitation number still increased. The fluctuations in the curves can possibly be explained by the variation in the flow field around the afterbody as the pitch angle is increased, Fig. 11.

The effects of cavitation number are apparent. The essential cause for the observed changes with increasing cavitation number are due to the decreased size of the cavity and the resultant increase in penetration of the afterbody into the water. The differences among the three models are due to the variation in the afterbody planing forces. The flat surface planing drag and lift coefficients for the A-4-5 and A-4-10 models are presented in Figs. 12 and 13. The line curves in these figures are the corresponding coefficients for the right circular cylinder planing on a flat surface[13].

It appears that the conical portions of the afterbodies definitely alter the planing coefficients.

METHOD OF PREDICTION OF COMPOSITE BODY FORCES

The general approach to the prediction of the composite body forces in full cavity flow is rather basic. It is simply to combine predicted nose forces with predicted afterbody forces. The nose forces for several conical noses including the flat disk are available in reference 2. The prediction of the afterbody forces is much more complex. First, the cavity shapes produced by the flat disk at an angle of attack were computed, reference 6, for several cavitation numbers. The cavity centerline was corrected for buoyancy effects as noted in reference 6. The model profile was then superimposed upon the predicted cavity shape at the specific angle of attack as shown in Fig. 14. From this figure the afterbody planing angle, submergence ratio, and lateral surface curvature ratio can be determined. The local angle between the afterbody and the cavity wall vary considerably along the wetted portion of the afterbody. Since no information exists on the effects of axial surface curvature, the planing angle has been defined as the angle between the model centerline and the cavity surface at the point on the surface which is normal to the lower edge of afterbody. This angle actually represents the maximum possible planing angle for the body. Any modification of this angle to include some of the effects of the lower planing angles forward of the base would have to be a complex correction involving the specific model shape and actual wetted length. Hence for simplicity and consistency the planing angle at the base was used.

The submergence ratio of the afterbody is similarly involved in the axial variation in local planing angle. Here again the limiting case at the base of the model was used. That is, the submergence is the distance along the normal line, indicated above, from the tip of the model base to the cavity surface.

The lateral surface curvature has been shown to have a large effect upon planing forces, Ref. 13. Since the cavity probably does not have a circular cross section at angles of attack, the local curvature on the

planing side of the cavity was used. The radius of the cavity wall was assumed to be equal to the displacement of the cavity wall from the cavity centerline. To be consistent with the above definitions the radius was measured at the axial station corresponding to the point used for the planing angle.

With the planing angle, submergence ratio, and lateral curvature ratio determined as functions of cavitation number the planing cylinder data from Ref. 13 were used to predict the afterbody forces. The planing cylinder data were used since they were the only available results showing the effects of lateral surface curvature.

The final composite forces were then obtained by adding the nose and afterbody forces. It should be noted that since most of the afterbody force data are presented in axes which are parallel and perpendicular to the free stream velocity, the planing data should be transferred from the system which is parallel to the cavity surface at the base to the axis system as used for the nose forces. Since the surface-to-free stream angles were on the order of a few degrees for these models, no transfer of axis systems was used.

Inasmuch as afterbody coefficient data for the models are definitely different from the cylinder data, an approximate analysis was made using the measured flat surface planing forces and correcting them by the values shown in Ref. 13 for the cylinders. Predicted coefficients were obtained at pitch angles of 0, 4, 8, 12, and 16 degrees.

Figure 15 shows the measured and predicted lift and drag coefficients for the A-4-5 model for a submergence of 0.25 feet. The predicted results were based on the actual cavitation numbers which corresponded to the given pitch angle. Figure 16 presents the measured and predicted force coefficients for the model A-4-10 as a function of cavitation number. These results are for both the forward and rear support points on the A-4-10 model.

COMPARISON OF PREDICTED AND EXPERIMENTAL RESULTS

Figures 15 and 16 present a comparison of the predicted lift and drag coefficients for the A-4-5 and A-4-10 models with the experimental results. It is apparent that predicted results based upon the planing cylinder afterbody do not satisfactorily describe the measured coefficients. The use of the actual afterbody planing data does tend to improve the comparison. However, there are still sizeable discrepancies between the observed and predicted results.

In the low angle of attack range, Fig. 16, it appears that the model drag is considerably larger than predicted, while only at 4 degrees is the lift larger than predicted. Because of the large axial curvature of the cavity wall, Fig. 14, the conical portion of the model actually planes through the cavity wall at angles and submergences previously defined for which the cone would not plane if it were on a flat surface. Hence for a comparable planing angle and submergence in the cavity the afterbody is actually experiencing forces on its conical portion which increase the drag and lift at these small angles. Thus it appears that a modification of the defined planing angle and submergence ratio to account for the axial curvature of the planing surface would be required before the predicted results could be expected to agree with the experimental data.

The two sets of data for the two different support points on the A-4-10 model, Fig. 16, suggest another reason for discrepancies in the results. It appears that there were definite tare loads imposed on the model strut by spray as a direct result of the planing process and that there was actually a flow of a thin sheet of water around the afterbody. In addition to the tare load due to the spray sheet hitting the strut, the disturbance of the spray field by the strut probably affected the forces on the downstream end of the body. Hence it appears that careful shielding and proper placing of the model support strut are very important considerations for model tests in full cavity flow.

It is of interest to note in Fig. 6 that, as would be expected, the apparent pitch angle for which the model intersects the cavity wall decreases

with increased cavitation number. However, the rate of decrease in intersection angle as a function of cavitation number is greater than that predicted by the cavity shape analysis based on Ref. 6. In fact, the discrepancy between the predicted and actual intersection angle decreases with the depth of submergence of the model below the water surface. Figure 17 presents the observed discrepancies and also the submergence on which the predicted results are based. It is assumed that there is a buoyant effect due to the free surface which increases the cavity centerline rise as the cavity approached the surface causing the model to intersect the cavity at a smaller than predicted angle. Hence, the predicted cavity wall should be corrected for the differences in the cavity centerline displacement as a function of the model depth. The predicted results shown in this report were not corrected for this depth effect because the large effects previously discussed would overshadow this correction.

A final experimental run was made using a 1-inch diameter disk and a 1-inch diameter cylindrical afterbody to eliminate some of the problems discovered in the original tests. Because of the model construction the runs were made at 7.8 and 12 degrees pitch angle with the cavitation number varying during the run. The lift and drag data for this model are shown in Fig. 18 along with the predicted results. This model combination eliminated the required extrapolation of the lateral curvature effects encountered with the previous models, reduced the extent of the axial curvature effects, eliminated spray impingement on the strut, and reduced the surface effects on the cavity by testing at a 0.50 and 0.70 feet submergence. The comparison of the experimental and predicted results is good.

TABLE I.

LIST OF SYMBOLS

A = Area of model base = $\frac{\pi d^2}{4}$, ft^2

d = Diameter of model base, ft

D = Diameter of cavity at base of model, ft

L_1 = Distance from base along model centerline to center of pressure of normal force, ft

P_k = Pressure in cavity, psia

P_o = Static pressure in free stream, psia

V = Velocity in free stream, fps

α = Angle of attack, degrees

δ = Distance model penetrates through planing surface, ft

ρ = Density of water, $slugs/ft^3$

C_D = Drag coefficient = $\frac{\text{Drag}}{\rho/2\ V^2\ A}$

C_L = Lift coefficient = $\frac{\text{Lift}}{\rho/2\ V^2\ A}$

C_M = Pitching moment coefficient = $\frac{\text{Pitching moment}}{\rho/2\ V^2\ A\ d}$

L_1/d = Center of pressure ratio = $\frac{\text{Pitching moment}}{d(\text{Drag} \sin \alpha + \text{Lift} \cos \alpha)}$

σ = Cavitation number = $\frac{P_o - P_k}{\rho/2\ V^2} \times 144$

LIST OF FIGURES

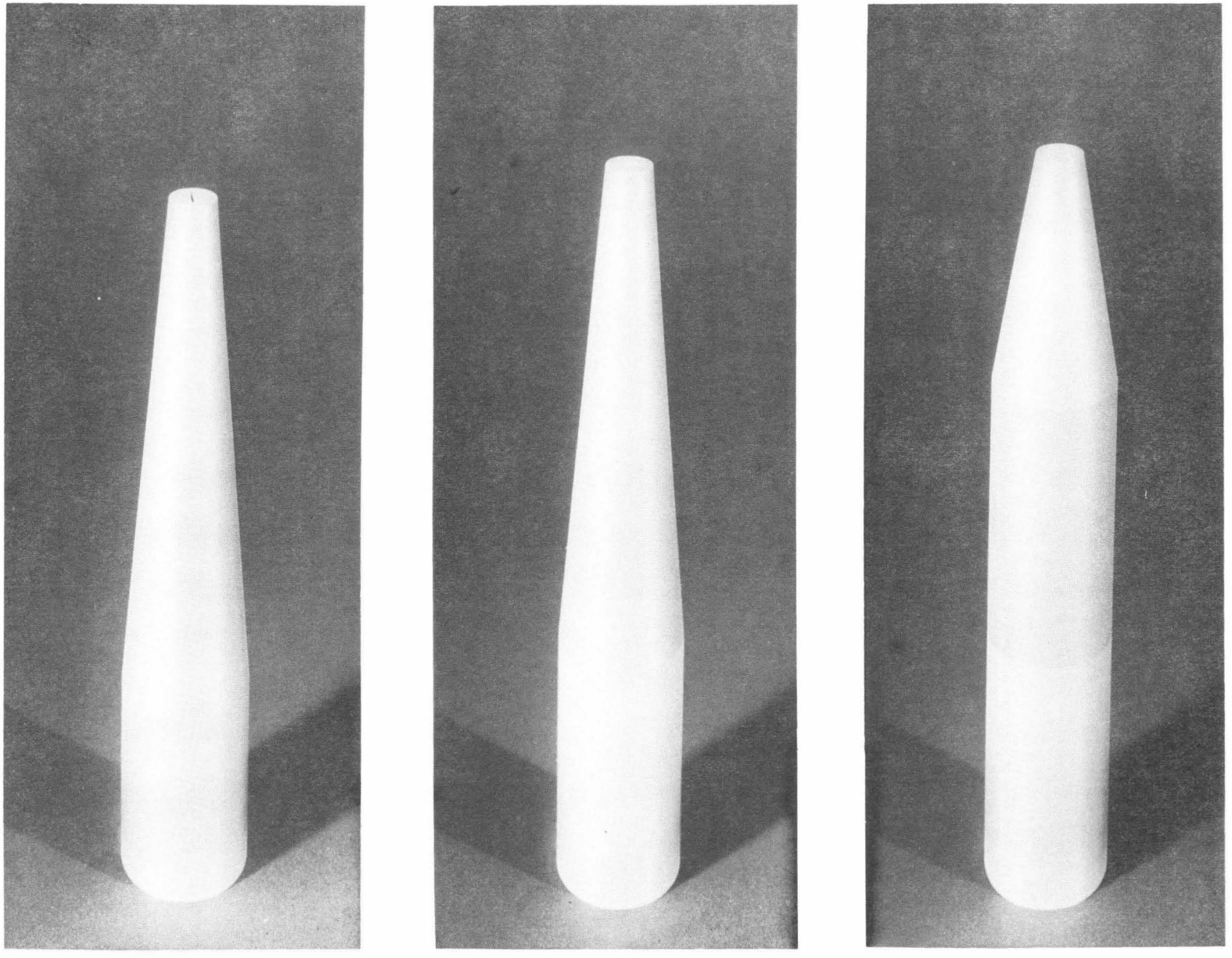

Fig. 1. Truncated cone cylinder models.

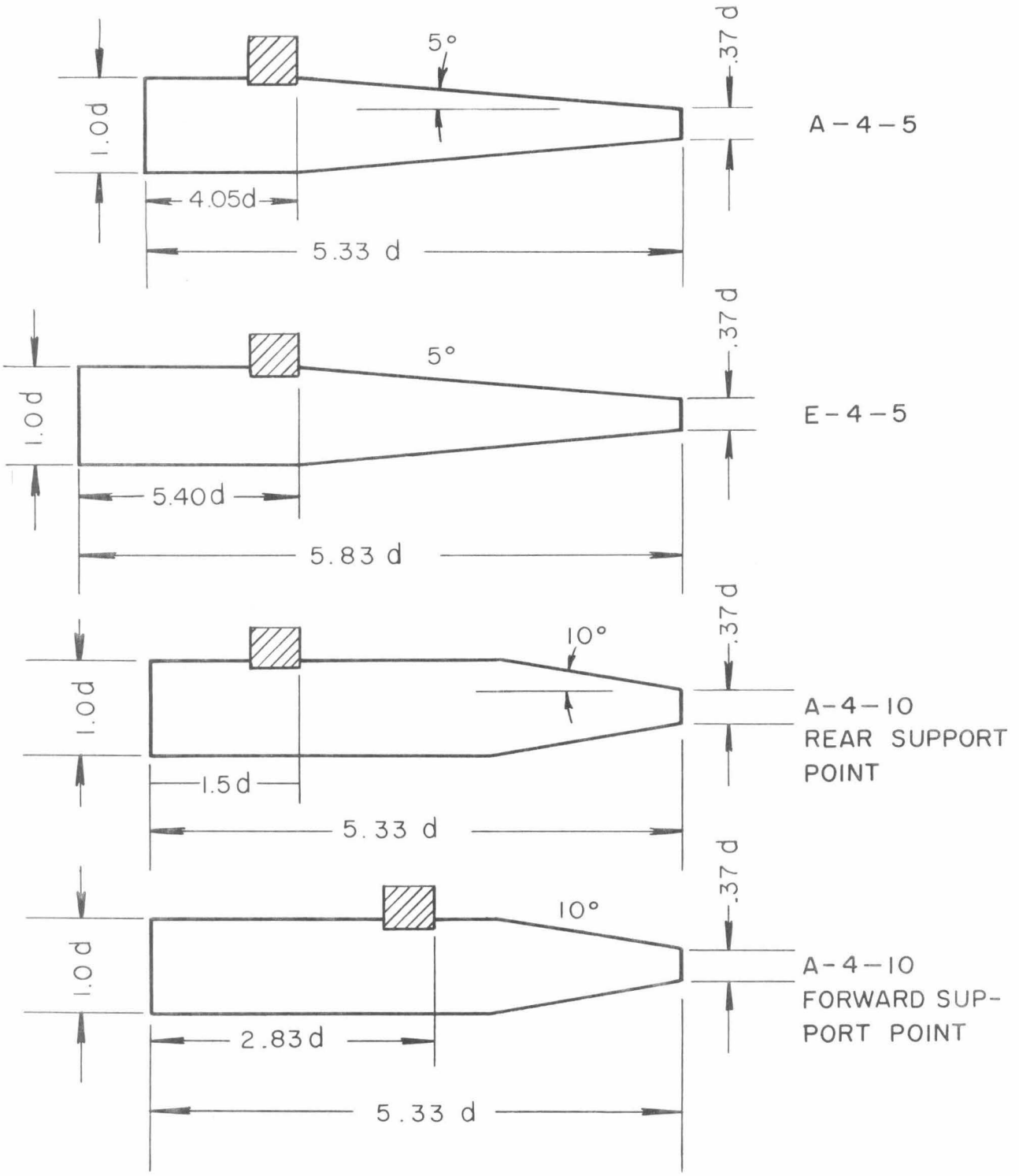

Fig. 2. Model designation and dimensions.

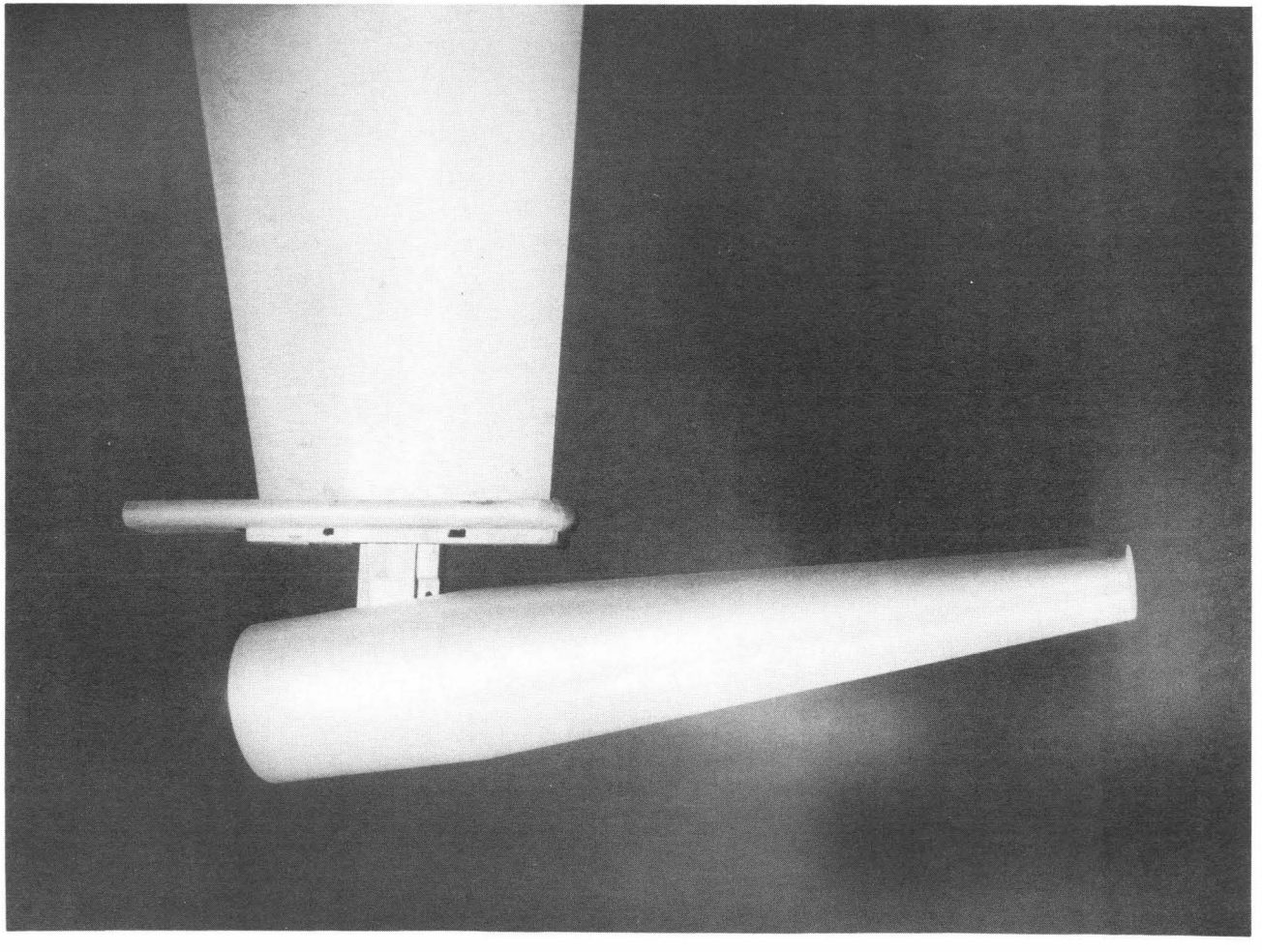

Fig. 3. Model installation on strut with shield.

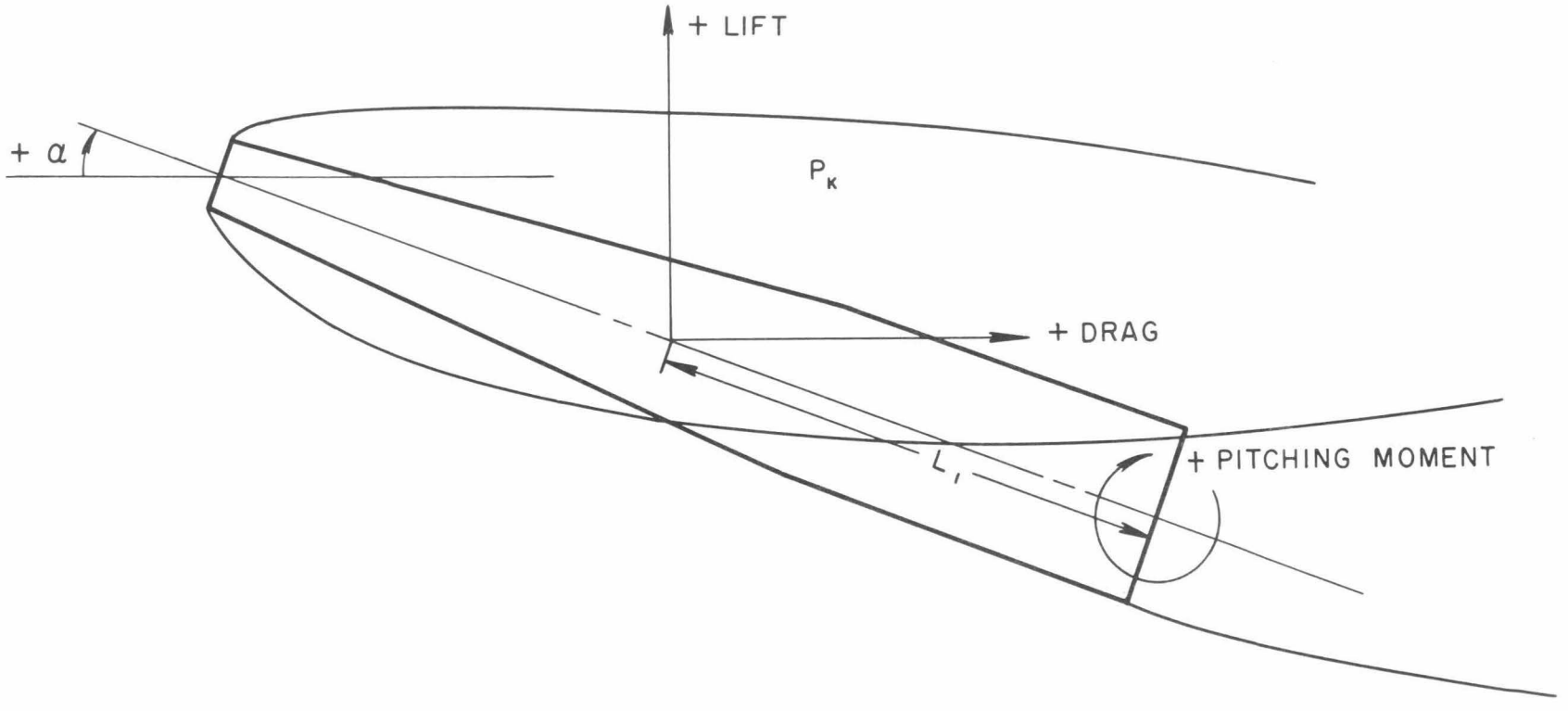

Fig. 4. Schematic of data sign conventions.

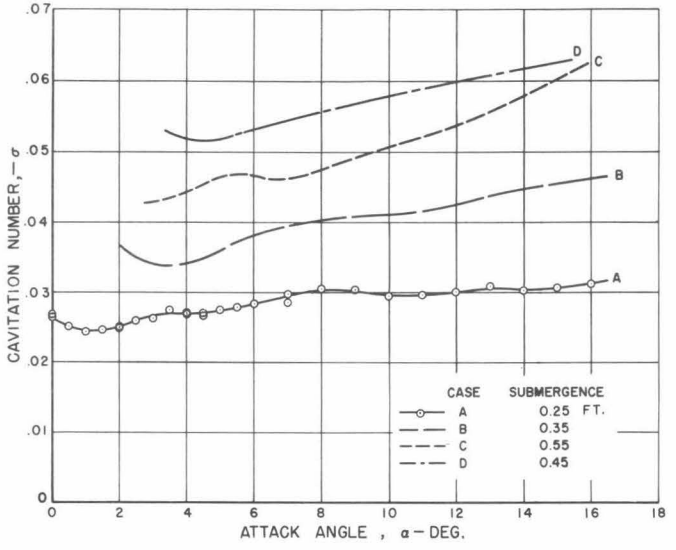

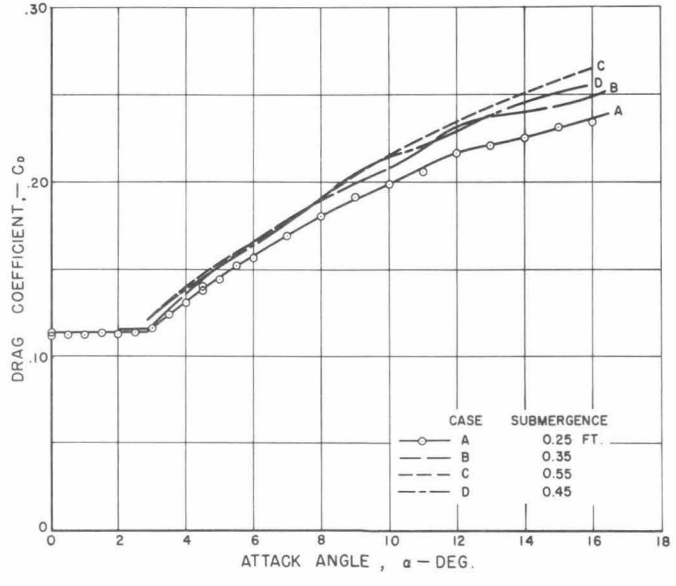

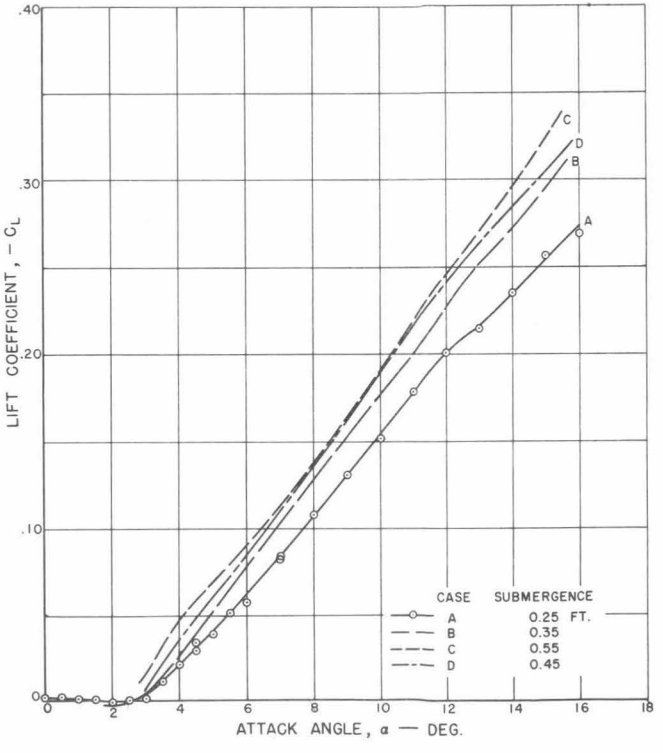

Fig. 5. Cavitation number, drag coefficient and lift coefficient for Model A-4-5.

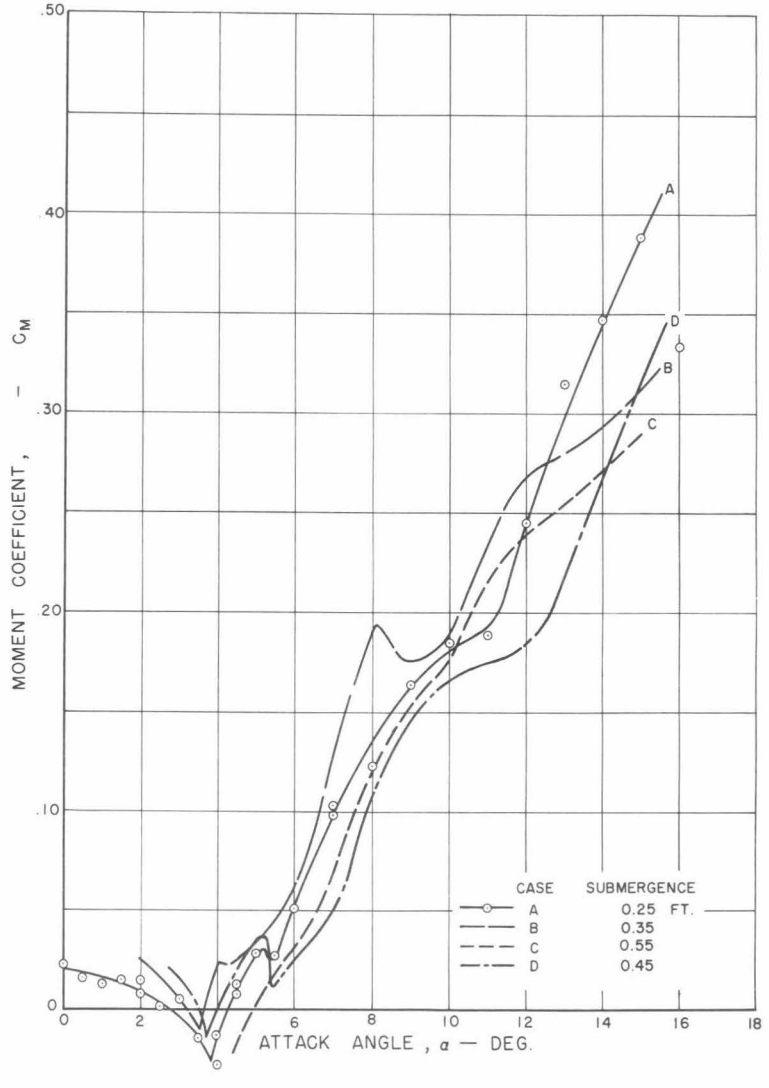

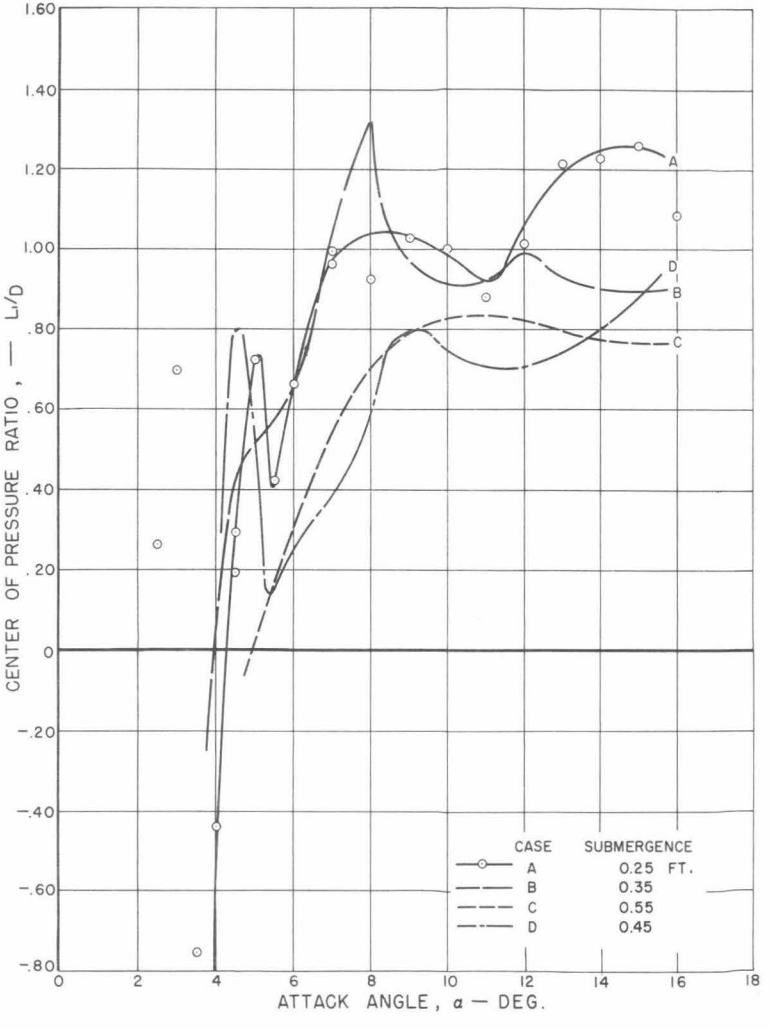

Fig. 6. Pitching moment coefficient and center of pressure ratio for Model A-4-5.

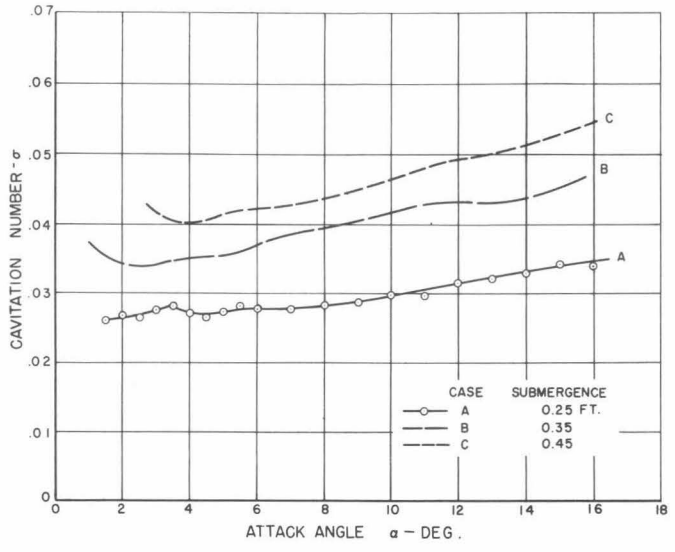

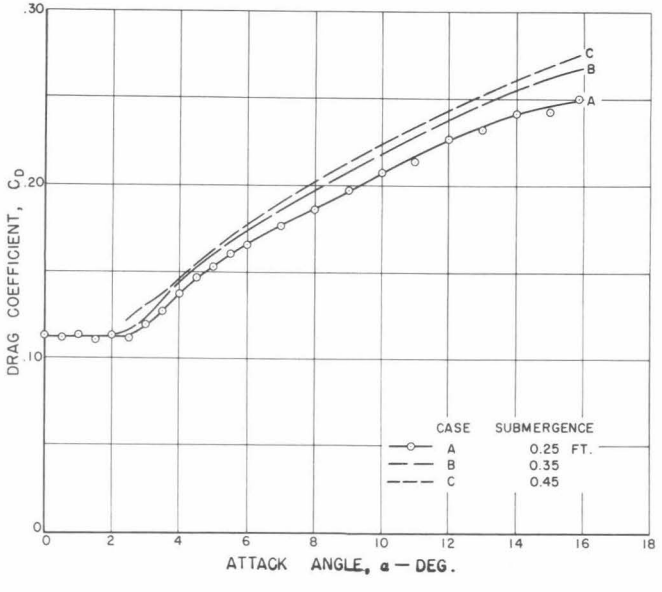

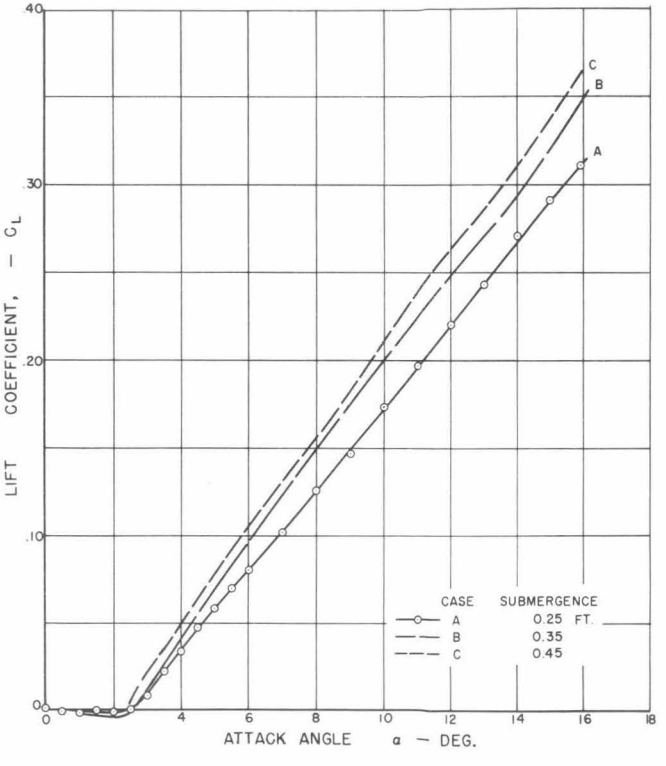

Fig. 7. Cavitation number, drag coefficient and lift coefficient for Model E-4-5.

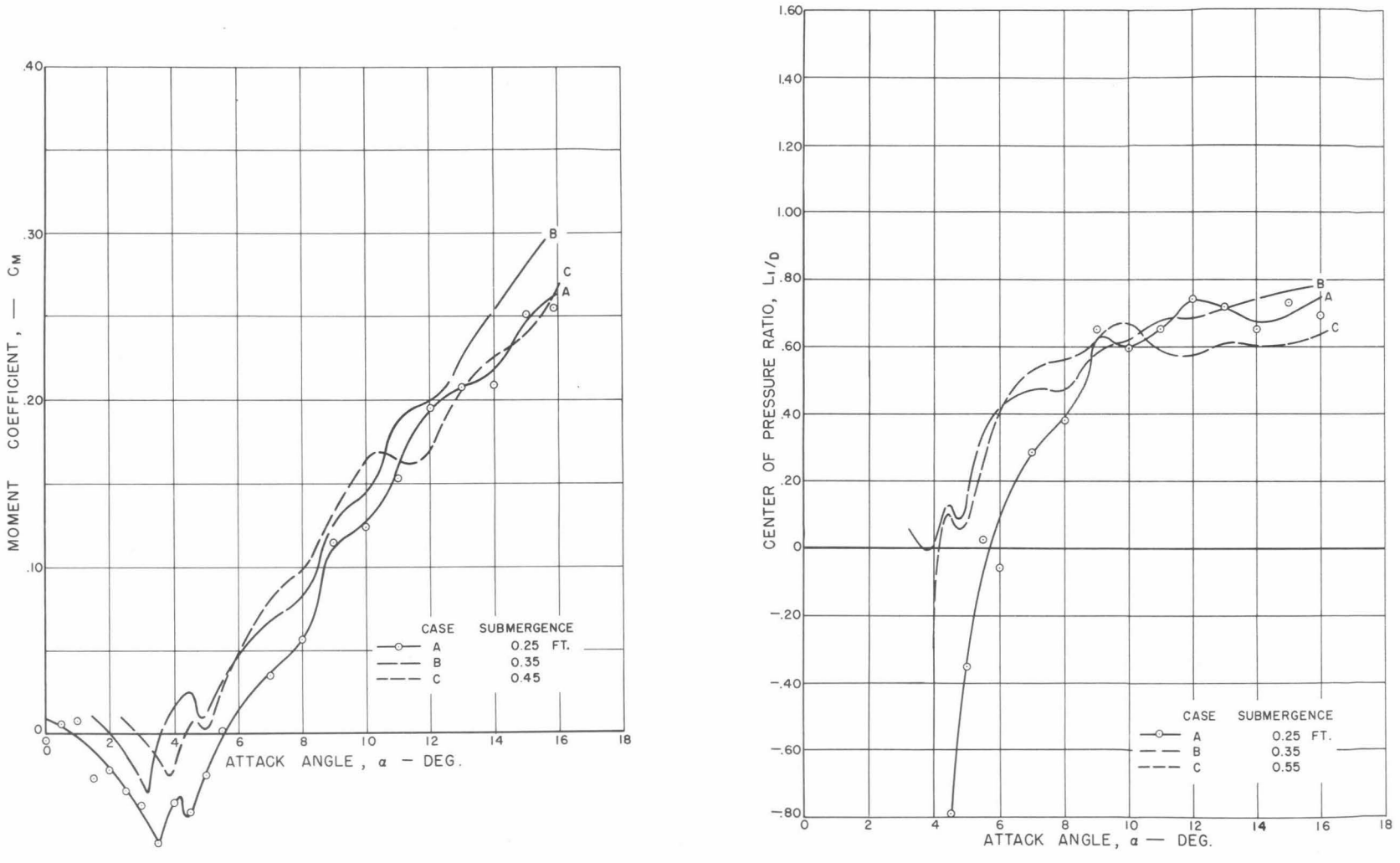

Fig. 8. Pitching moment coefficient and center of pressure for Model E-4-5.

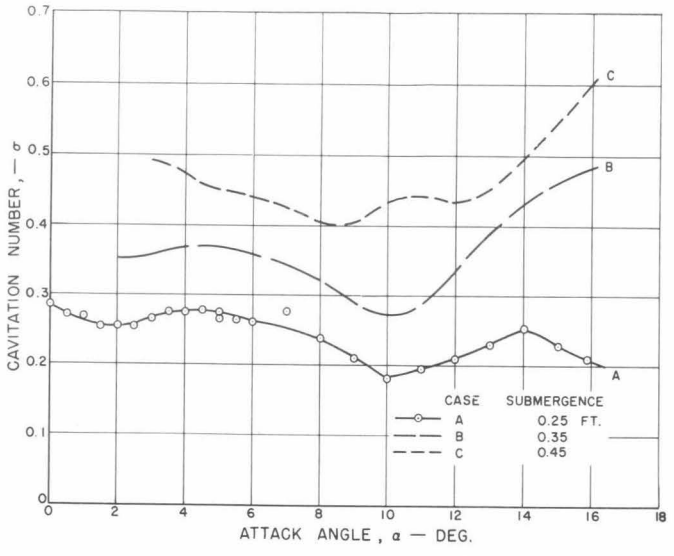

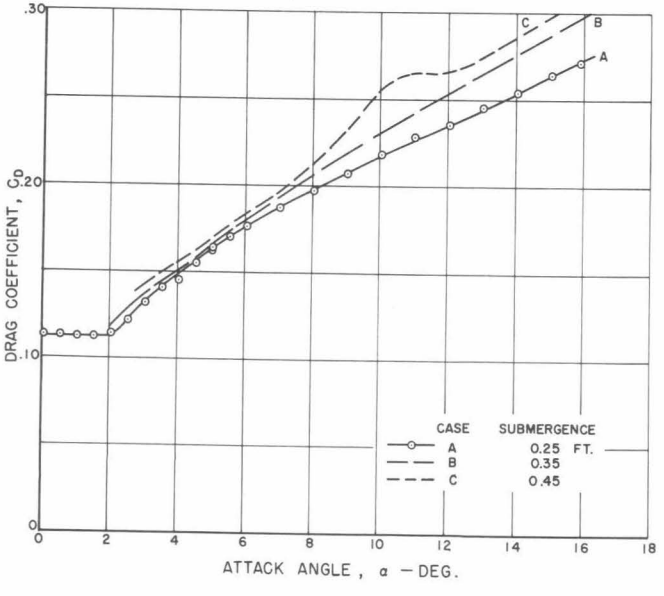

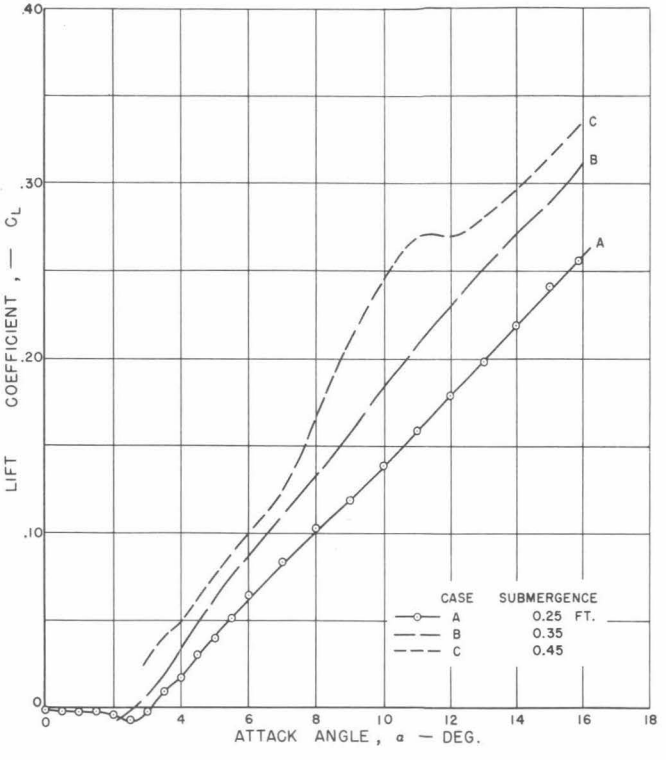

Fig. 9. Cavitation number, drag coefficient and lift coefficient for Model A-4-10.

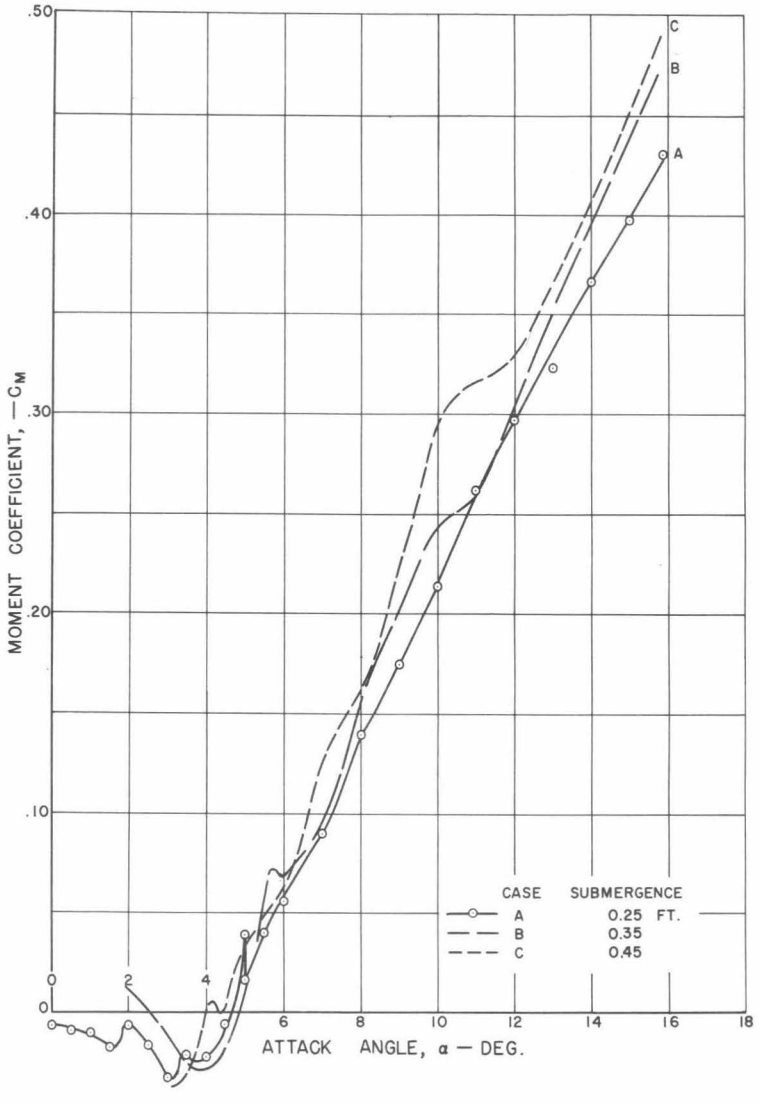

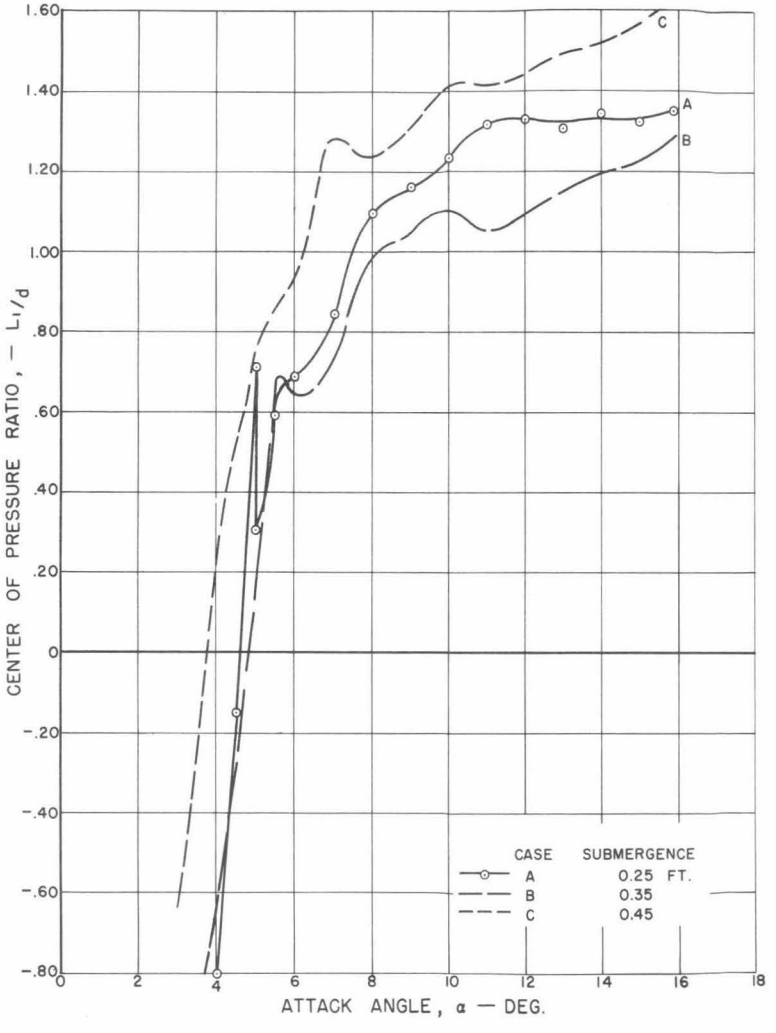

Fig. 10. Pitching moment coefficient and center of pressure ratio for Model A-4-10.

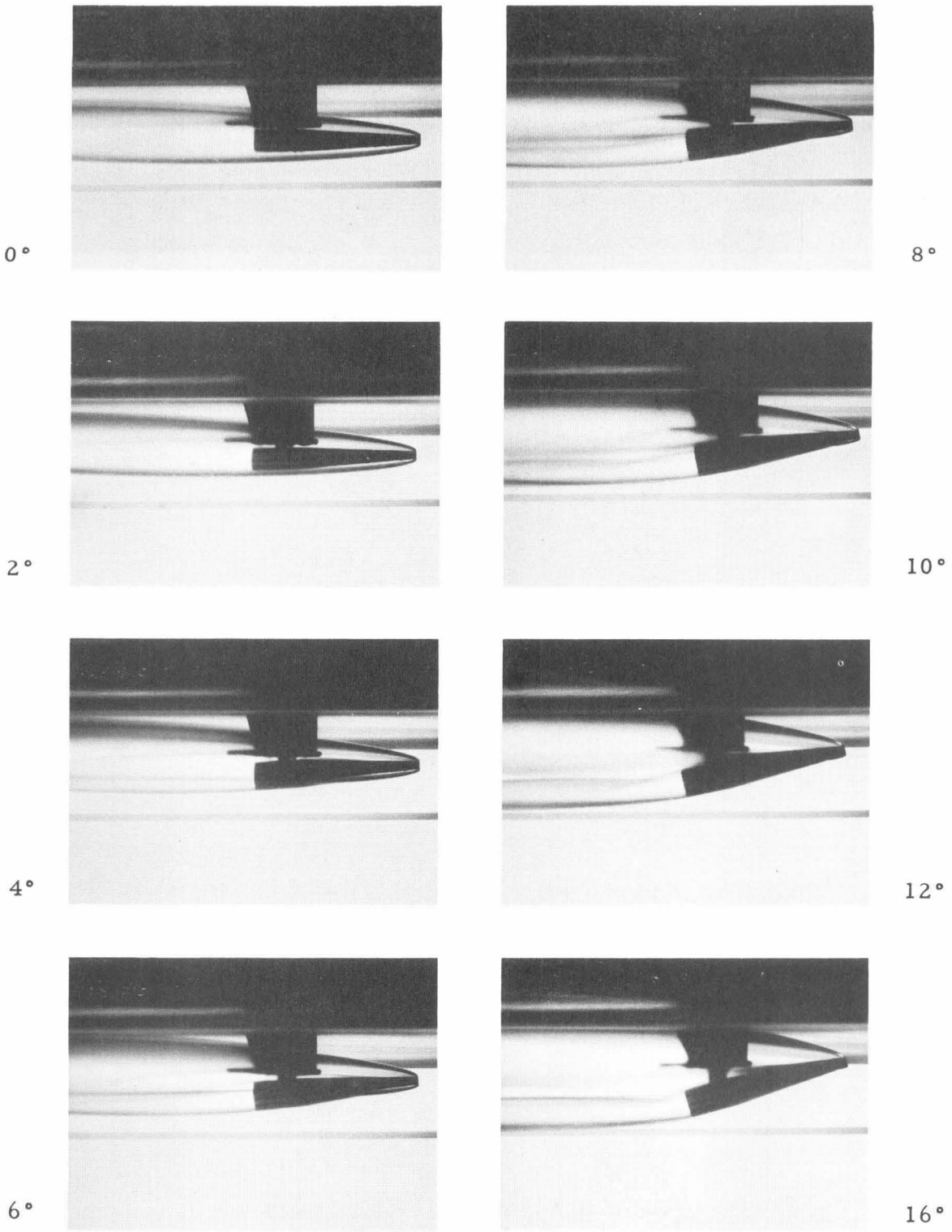

Fig. 11. Photographs of full cavity flow of Model A-4-5 for submergence of 0.25 feet.

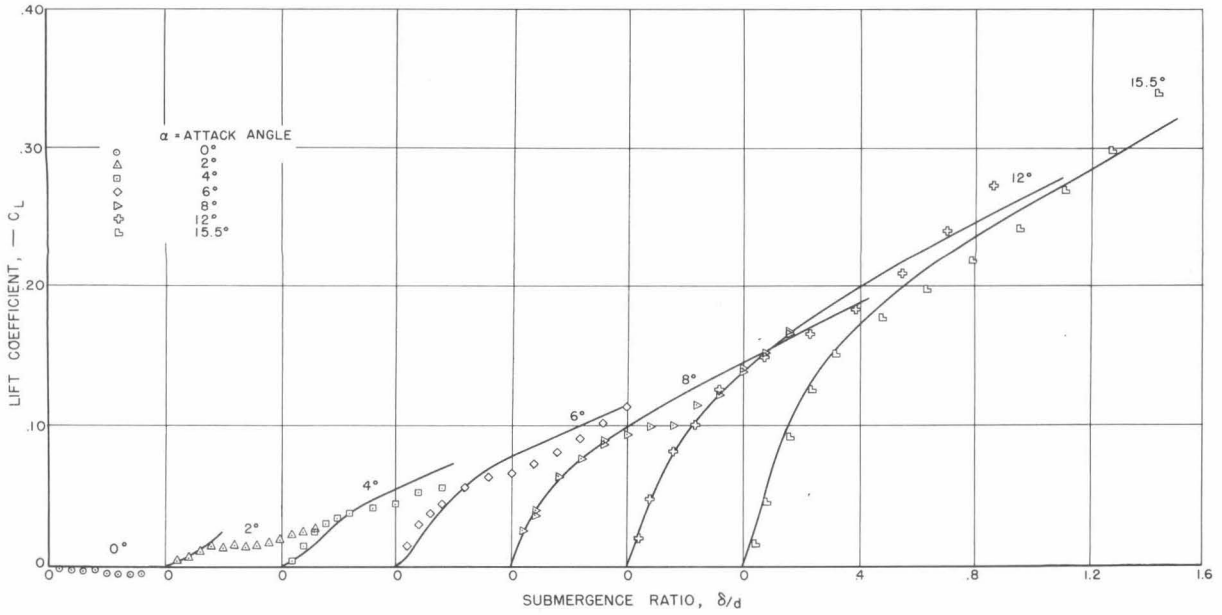

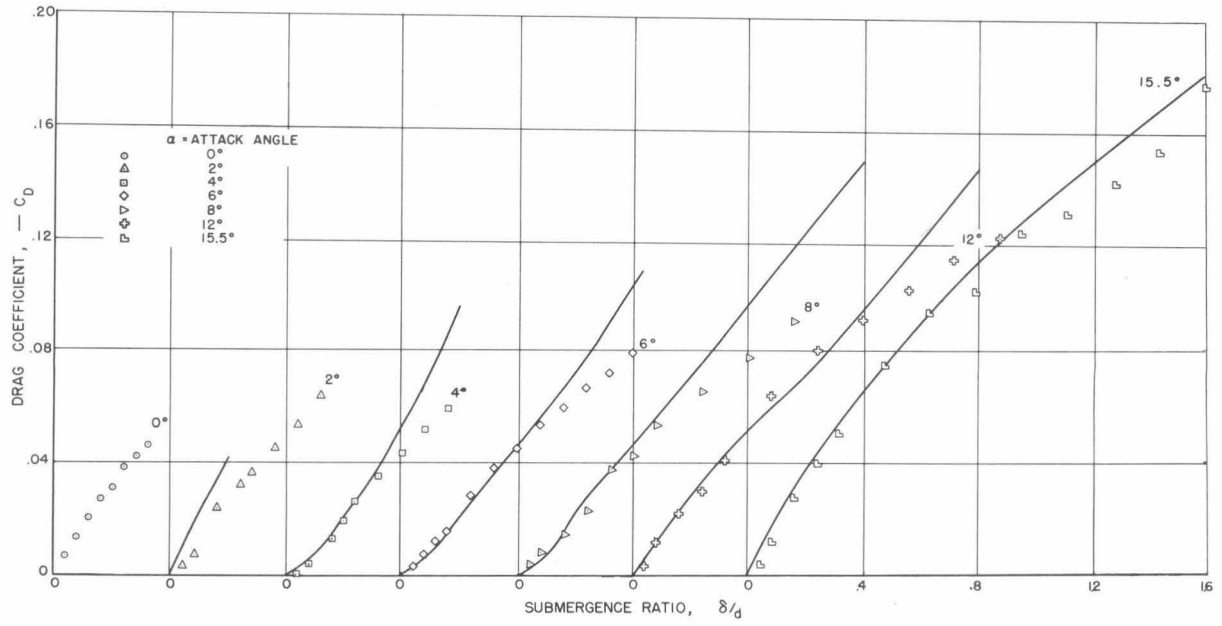

Fig. 12. Flat surface planing lift and drag coefficients for Model A-4-5 and cylinder.

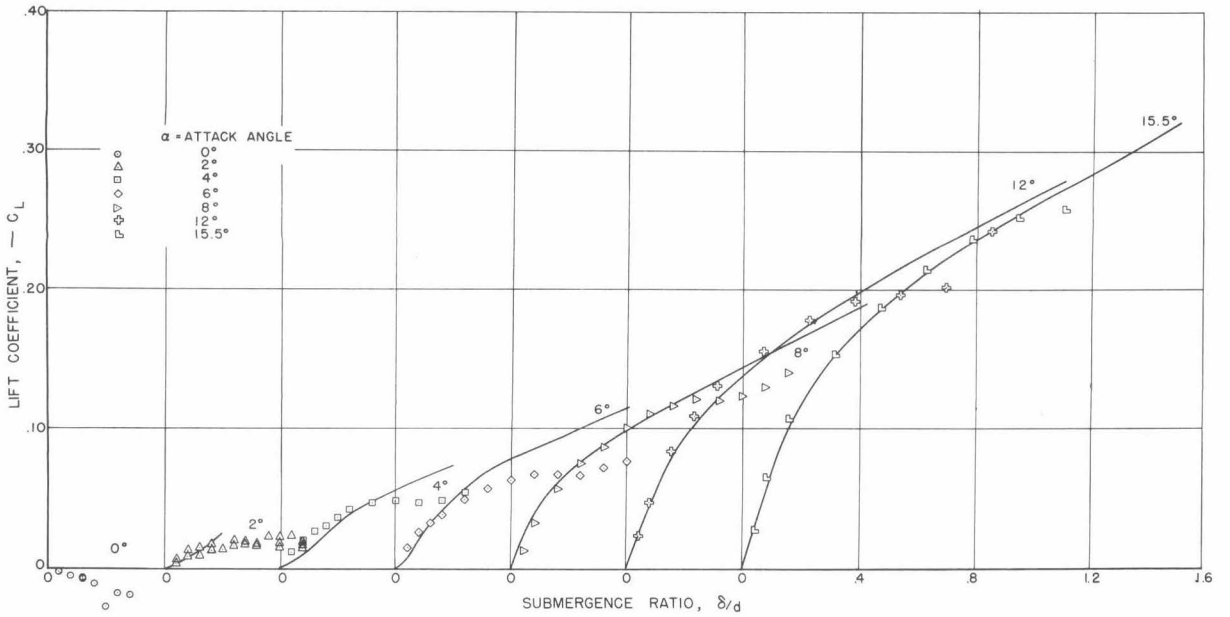

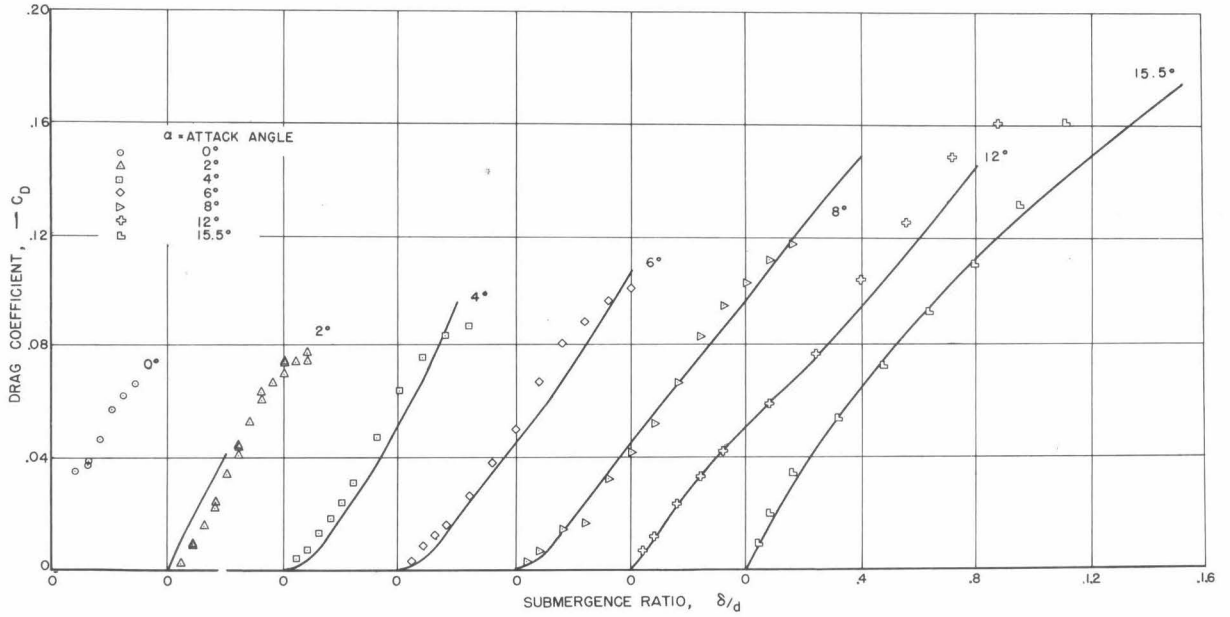

Fig. 13. Flat surface planing lift and drag coefficients for Model A-4-10 and cylinder.

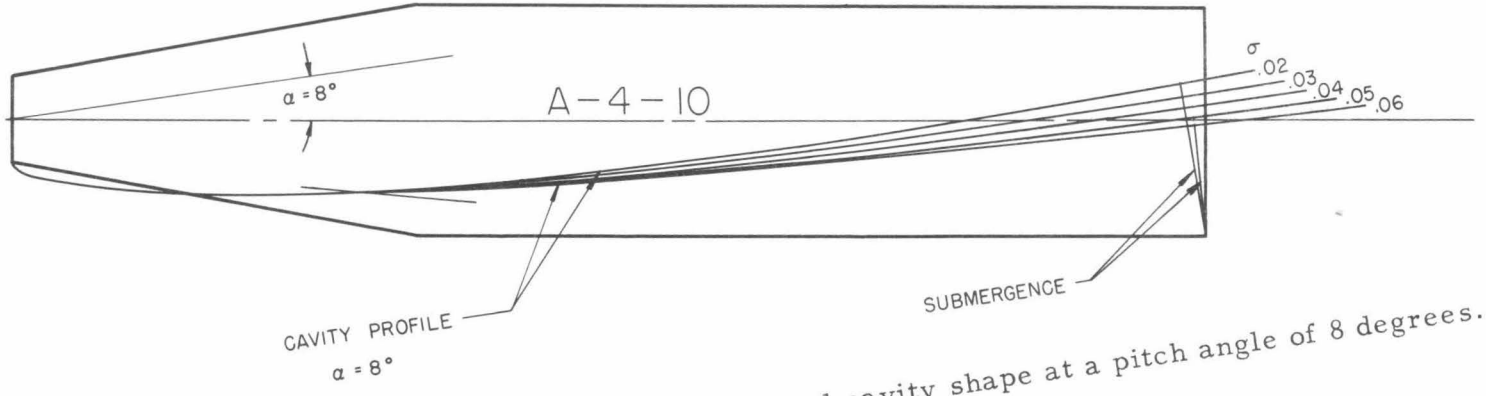

Fig. 14. Profile of Model A-4-10 with predicted cavity shape at a pitch angle of 8 degrees.

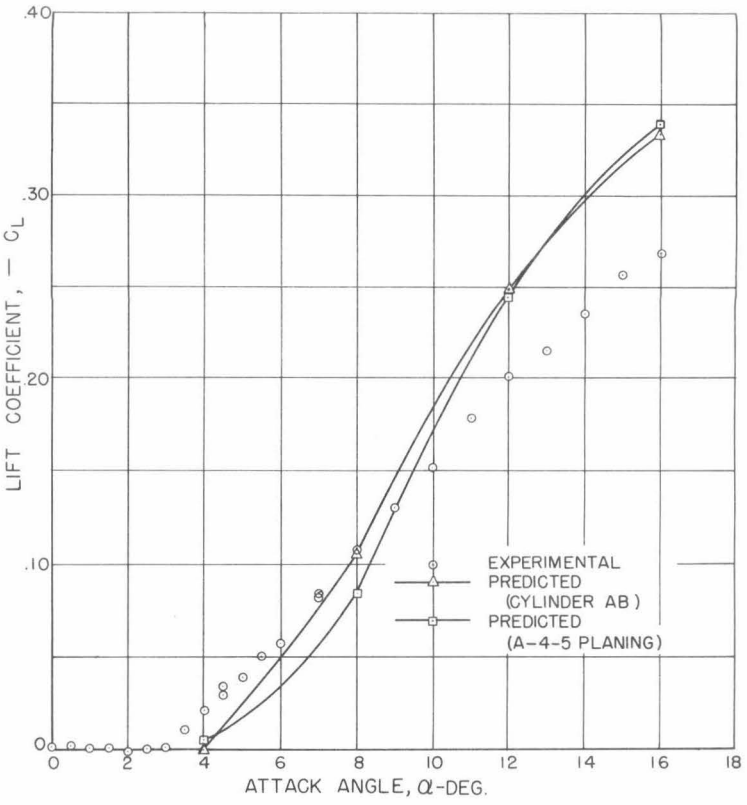

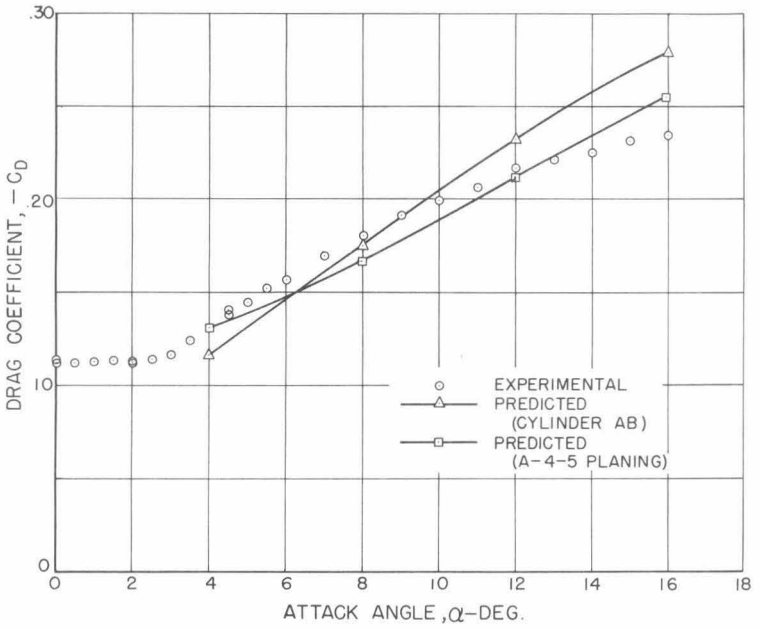

Fig. 15. Measured and predicted lift and drag coefficients for A-4-5 at 0.25 feet submergence.

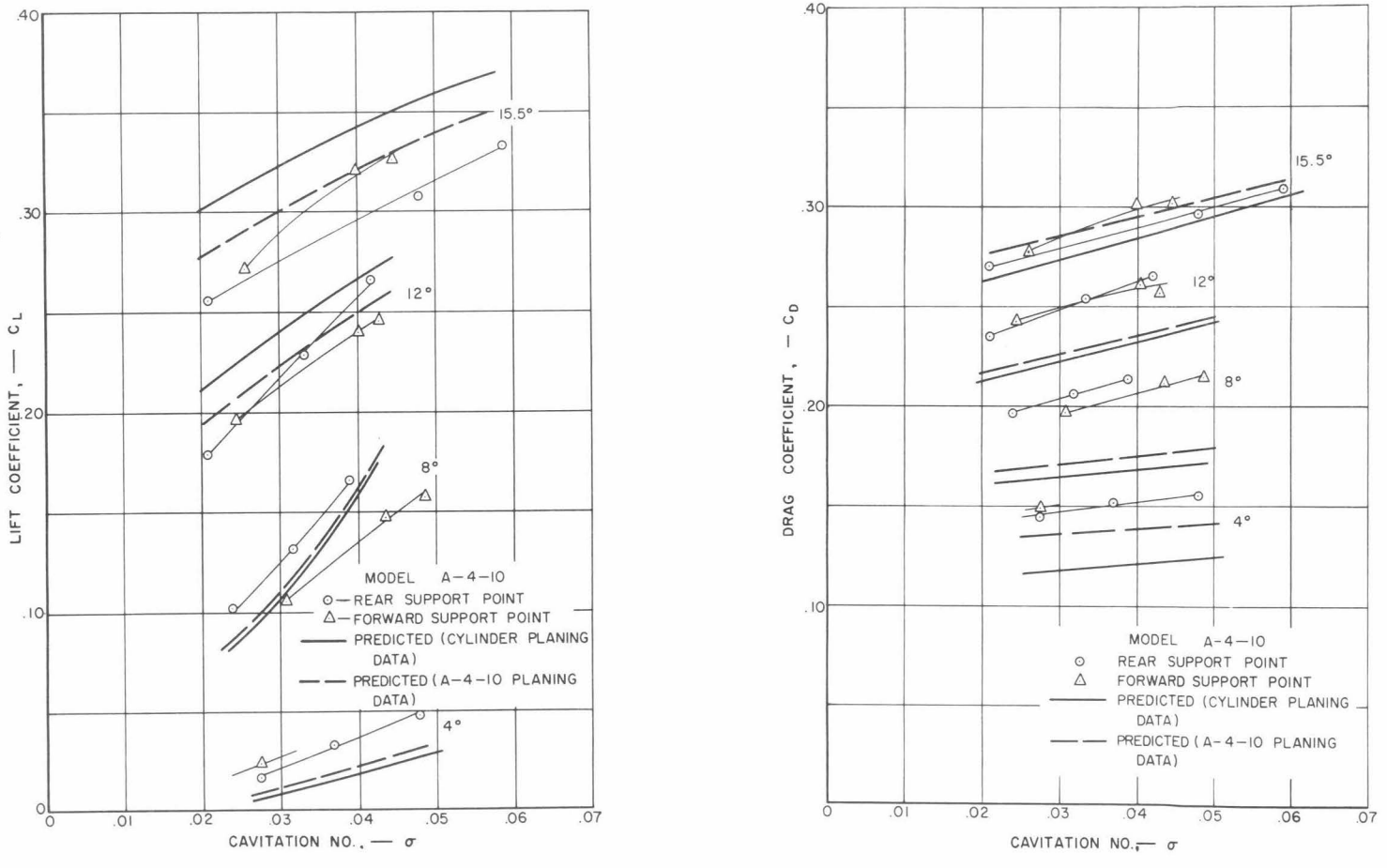

Fig. 16. Measured and predicted lift and drag coefficients for A-4-10 as a function of cavitation number for forward and rear support points.

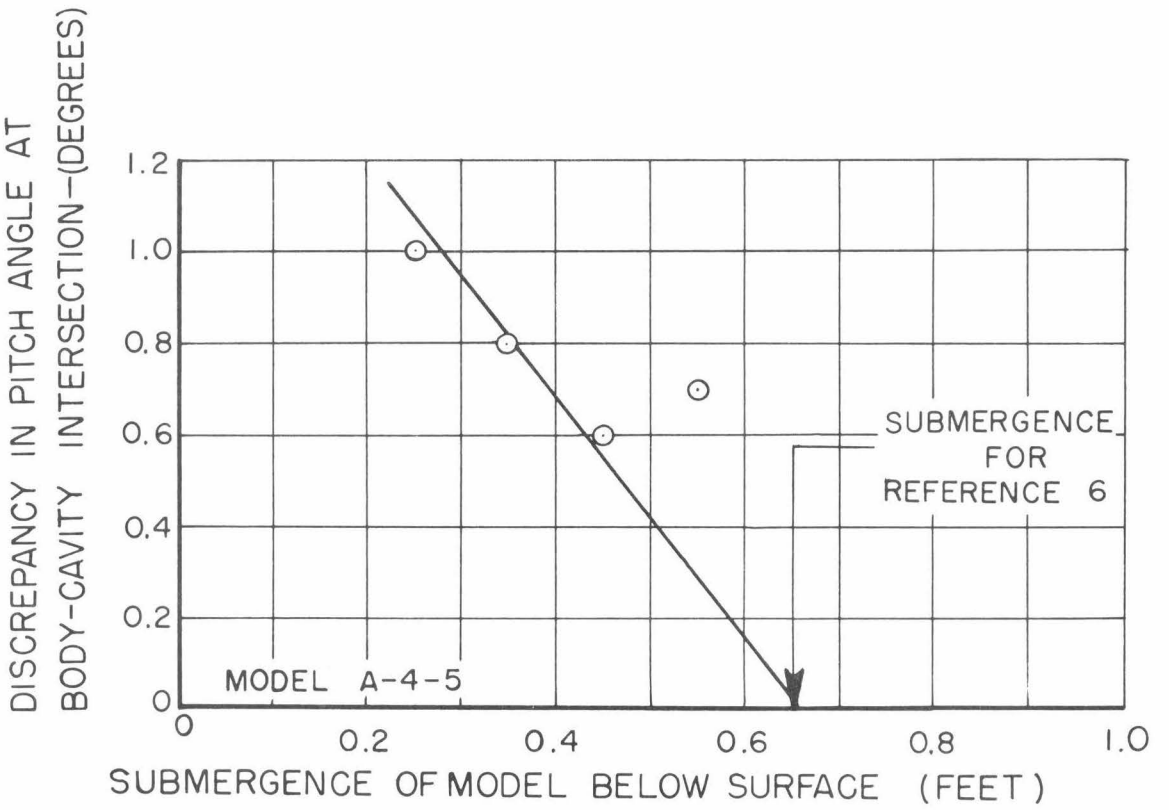

Fig. 17. Discrepancy in pitch angle at body-cavity intersection (Model A-4-5).

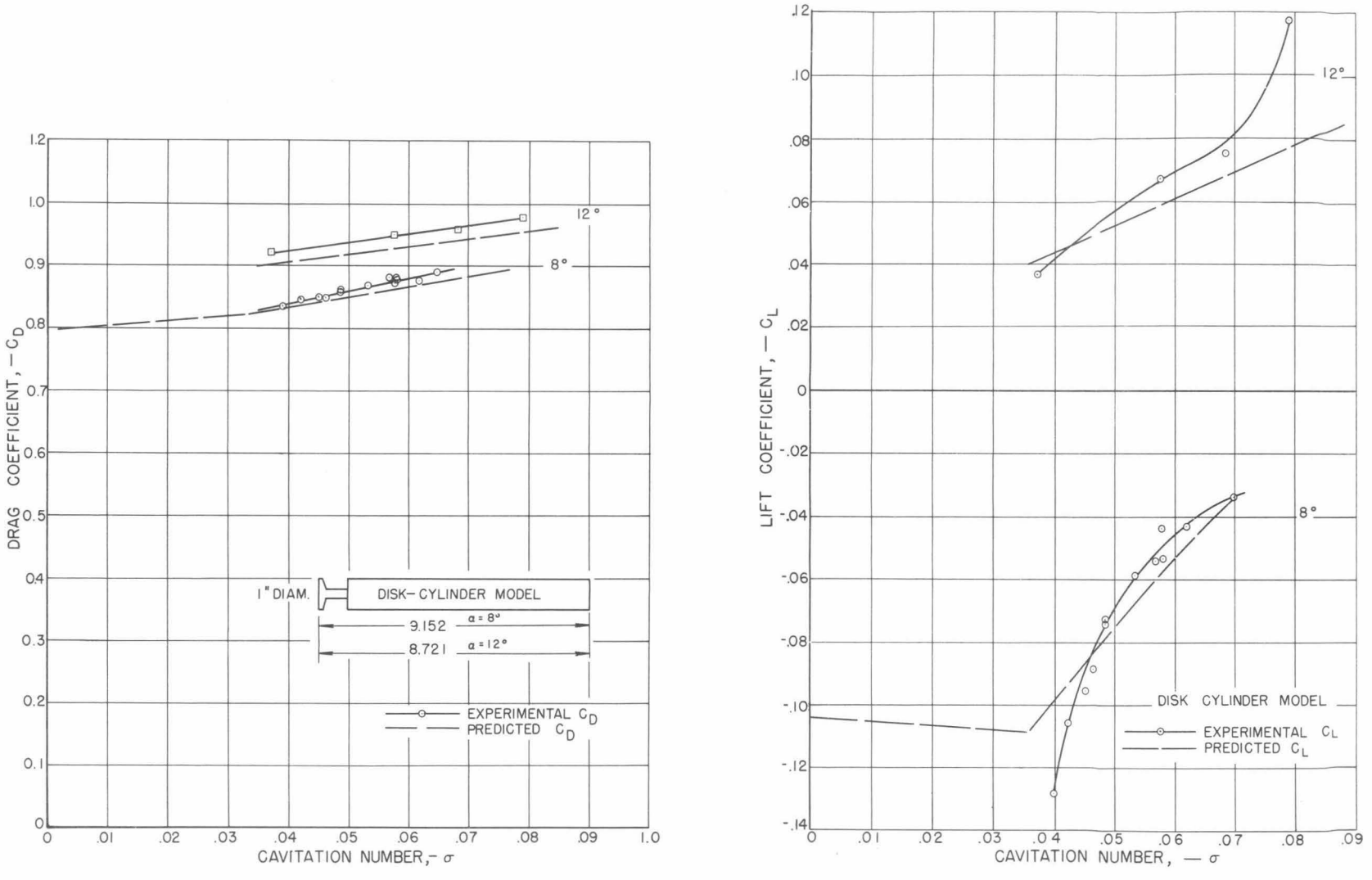

Fig. 18. Measured and predicted lift and drag coefficients for 1-inch diameter disk nose and 1-inch diameter cylinder afterbody model.

BIBLIOGRAPHY

1. Knapp, R. T., Levy, J., O'Neill, J. P., and Brown, F. B., "The Hydrodynamics Laboratory of the California Institute of Technology", Trans. ASME, July 1948.

2. Kiceniuk, T., "An Experimental Study of the Hydrodynamic Forces Acting on a Family of Cavity-Producing Conical Bodies of Revolution Inclined to the Flow", California Institute of Technology, Hydrodynamics Laboratory Report No. E-12.17, June 1954.

3. O'Neill, J. P., "Flow Around Bodies with Attached Open Cavities", California Institute of Technology, Hydrodynamics Laboratory Report No. E-24.7, December 1954.

4. Perry, Byrne, "Evaluation of the Integrals Occurring in the Cavity Theory of Plesset and Shaffer", California Institute of Technology, Hydrodynamics Laboratory Report No. 21-11, December 1952.

5. Perry, B., and Hsu, En-Yun, "Water Tunnel Experiments on Spheres in Cavity Flow", California Institute of Technology, Hydrodynamics Laboratory Report No. E-24.9, April 1954.

6. Waid, R. L., "Cavity Shapes for Circular Disks at Angles of Attack", California Institute of Technology, Hydrodynamics Laboratory Report No. E-73.4, September 1957.

7. Swanson, W. M., and O'Neill, J. P., "The Stability of an Air-Maintained Cavity Behind a Stationary Object in Flowing Water", California Institute of Technology, Hydrodynamics Laboratory Memo Report No. M-24.3, September 1951.

8. Kiceniuk, T., "Experimental Study of Froude Number Modeling for Cylinders Planing on Water", California Institute of Technology, Hydrodynamics Laboratory Report No. E-24.4, January 1952.

9. Kiceniuk, T., and Greengard, R., - - - - - - California Institute of Technology, Hydrodynamics Laboratory Report No. E-12.3. January 1952. (CONFIDENTIAL)

10. Greengard, R.- - - - - California Institute of Technology, Hydrodynamics Laboratory Report No. E-12.9. August 1952. (CONFIDENTIAL)

11. Kiceniuk, T., "Force and Moment Measurements on a Torpedo Afterbody with Three Tail Configurations Planing on a Free Water Surface", California Institute of Technology, Hydrodynamics Laboratory Report No. E-54, December 1953.

12. Kermeen, R. W., "Forces on a Cylinder Planing in a Vapor Cavity", California Institute of Technology, Hydrodynamics Laboratory Report No. E-12.14, November 1953.

BIBLIOGRAPHY
(Cont'd)

13. Waid, R. L., and Kermeen, R. W., "Forces on Cylinders Planing on Flat and Curved Surfaces in Cavitating and Noncavitating Flow", California Institute of Technology, Hydrodynamics Laboratory, Report No. E-73.5, September 1957.

14. Waid, R. L., "Force Coefficients of Six Related Body Configurations in Cavitating Flow", California Institute of Technology, Hydrodynamics Laboratory Report No. E-51-1. January 1954.

15. Kiceniuk, T., - - - - - - California Institute of Technology, Hydrodynamics Laboratory Memorandum Report No. EM-12.15, October 1953. (CONFIDENTIAL)

16. Mosteller, G. G., - - - - - - U. S. Naval Ordnance Test Station, NOTS 302, 14 July 1950. (NAVORD Report 1240) (CONFIDENTIAL)

17. - - - - - - Worcester Polytechnic Institute, Alden Hydraulic Laboratory, WPI, Report No. 27. (CONFIDENTIAL)

DISTRIBUTION LIST

Copy No.	
1-4	Chief, Bureau of Ordnance, Navy Dept., Washington 25, D. C. Attn: Code ReO-3
5-8	Chief, Bureau of Ordnance, Navy Dept., Washington 25, D. C. Attn: Code ReU
9-10	Chief, Bureau of Ordnance, Navy Dept., Washington 25, D. C. Attn: Code Ad3
11-13	Chief, Bureau of Aeronautics, Navy Dept., Washington 25, D. C.
14-18	Chief, Bureau of Ships, Navy Dept., Washington 25, D. C.
19-21	Chief, Office of Naval Research, Navy Dept., Washington 25, D. C. Attn: Code 438
22	Commanding Officer, Office of Naval Research Branch Office, 1030 East Green Street, Pasadena 1, California
23-24	Commanding Officer and Director, David Taylor Model Basin, Washington 7, D. C.
25-26	Commanding Officer, U. S. Naval Underwater Ordnance Station, Newport, Rhode Island
27-28	Commander, U. S. Naval Ordnance Laboratory, White Oak, Silver Spring, Maryland
29-30	Commander, U. S. Naval Ordnance Test Station, Pasadena, California
31	Commander, U. S. Naval Ordnance Test Station, China Lake, California
32	Director, Experimental Towing Tank, Stevens Institute of Technology, via: Bureau of Aeronautics Representative c/o Bendix Aviation Corp., Eclipse-Pioneer Division, Teterboro, New Jersey
33	Director, Ordnance Research Laboratory, Pennsylvania State University, University Park, Pennsylvania
34	Alden Hydraulic Laboratory, Worcester Polytechnic Institute, Worcester, Mass., via: Inspector of Naval Material, 495 Summer Street, Boston 10, Mass.
35-36	Librarian, U. S. Naval Postgraduate School, Monterey, Calif.

DISTRIBUTION LIST (cont'd)

Copy No.	
37-46	British Joint Services Mission, Navy Staff, via: Chief, Bureau of Ordnance, Navy Dept., Washington 25, D. C., Attn: Code Ad8
47-49	Commander, U. S. Naval Proving Ground, Dahlgren, Virginia
50-51	National Advisory Committee for Aeronautics, Langley Memorial Aeronautical Laboratory, Langley Field, Virginia
52	National Advisory Committee for Aeronautics, Lewis Flight Propulsion Lab., Cleveland Airport, Cleveland, Ohio
53	Director, National Advisory Committee for Aeronautics, 1512 H Street, N. W., Washington 25, D. C.
54	Director, National Advisory Committee for Aeronautics, Ames Laboratory, Moffett Field, California
55-56	Commander, Air Research and Development Command, Post Office Box 1395, Baltimore 3, Maryland
57	ASTIA Reference Center, Technical Information Division, Library of Congress, Washington 25, D. C.
58-63	Director, Armed Services Technical Information Agency, Documents Service Center, Knott Building, Dayton 2, Ohio. Attn: DSC-SA